Cooperative few-level fluctuations in coupled quantum systems

H. Körner and G. Mahler
Institut für Theoretische Physik, Universität Stuttgart, Pfaffenwaldring 57, 7000 Stuttgart 80, Germany
(Received 9 November 1992)

Fluctuations and noise are typical features of mesoscopic systems. Here we study the quantum-stochastic dynamics of an interacting network of local few-level subsystems. Controlled by the environment, this network is shown to exhibit a large repertoire of different behavioral patterns, including uncorrelated and correlated "quantum jumps": Such cooperation should be generic for certain networks and expected, e.g., also for various optically driven quasimolecular structures. When applied to a defect network controlling the current through a small tunnel junction, large-amplitude two-level current fluctuations appear, in agreement with experiment.

PACS number(s): 05.40.+j, 05.50.+q, 71.50.+t, 72.70.+m

I. INTRODUCTION

In the last few years various experiments confirmed that the time development of open quantum systems is inherently stochastic. Direct evidence is provided by the observation of "random telegraph signals" (RTS's), where observables (e.g., fluorescence intensity or electric current) fluctuate between few distinct values [1–9]. As a consequence one has to assume that the system itself evolves stochastically and "jumps" between discrete quantum levels [10,11]. This observation of "quantum jumps" has intimately been connected with the possibility to prepare and investigate individual quantum systems: Examples are the study of single ions in a Paul trap [1–3] or the spectroscopy of single dopant molecules in a host crystal in the wings of the inhomogeneously broadened line [12,13]. The reason is that in an ensemble of N *noninteracting* subsystems, each subsystem jumps independently (cf. Ref. [3]) and the superposition of many RTS's implies fluctuations decreasing with increasing N. Unfortunately, many large systems tend to behave like such an "independent ensemble," e.g., a gas of atoms or elementary excitations within a single crystal.

However, there are experimental indications that in an ensemble of *interacting* subsystems the RTS's of the constituents influence one another and thus give rise to considerably more complex random telegraph noise. An example is current fluctuations in small electronic devices [7,14]. They may be interpreted as being due to the influence of defects residing in two alternate states [6]. Most impressive is the observation of large-amplitude two-level RTS's which cannot be explained as the effect of a single defect. Even the so-called burst-noise phenomena [15] appear to fall into this category. Though mechanisms for synchronizing in the form of (electric or elastic) dipole interactions have been proposed [6,7], no model to explain the detailed dynamics appears to exist up to now.

The recent progress in nanostructure technology aimed at the structural control of artificial quantum systems (e.g., quantum dots in semiconductor materials [16–18]) is promising in this connection: It should become possible to adjust parameters (e.g., energy scales or transition rates) and tailor properties in order to optimize the quantum system for the observation of stochastic dynamics. We expect that complex stochastic behavior should become controllable in so-called quantum networks, arrays of interconnected quantum objects, realized, e.g., by charge-transfer quantum dots [19]. Quantum networks are also appealing in connection with prospective applications of synthetic nanostructures as "quantum functional devices" [20]: The challenge is to have quantum noise controlled and represent computer function.

In an ensemble description, the dynamics of an open quantum system is governed by a generalized master equation for the density matrix [21]. Its continuous time development, however, cannot explain the occurrence of quantum jumps. Extending this formalism to correlation functions merely allows us to describe fingerprints of the underlying stochastic dynamics in an averaged form [22,23].

In an alternative approach the stochastic process itself is taken as the starting point: Under certain conditions [24,25] or, more generally, by transforming onto the instantaneous diagonal representation [10], the generalized master equation reduces to a rate equation (Pauli master equation). The stochastic process can then easily be derived if one postulates that the corresponding Markoff process describes the "real" dynamics of the quantum object as continuously registered by the environment [10]. Correlation properties are included in this approach and emerge after averaging over the respective stochastic process. Similar goals, though for different scenarios, have been pursued in Ref. [11]. Both these approaches differ in the way coherence is incorporated, but should coincide if such effects can be neglected.

In this paper we apply the stochastic approach to quantum-network models in order to demonstrate the origin of complex RTS's and correlated quantum jumps. These models consist of localized few-level subsystems ("network nodes") that interact among one another through a diagonal energy renormalization. Coupling to the environment leads to a stochastic dynamics described by a rate equation in the high-dimensional network state

 ©1993 The American Physical Society

space. We consider two different boundary conditions (environments). The first one is a model of interacting two-level traps in a heat bath. The second one is a charge-transfer quantum dot array in an incoherent electromagnetic field as prototype for a synthetic quantum network. The dynamical repertoire of the second model is even larger as transition rates can be adjusted by the light field. Under certain restrictions ("detailed balance") it can be mapped onto our first model.

Our paper is organized as follows. In Sec. II we describe the general network model and derive its stochastic dynamics. Two different network realizations are introduced in Sec. III. In Sec. IV we consider various topologies: For two coupled two-level systems we demonstrate how complex stochastic behavior may emerge. We then go on to show how correlated quantum jumps may explain the occurrence of large amplitude RTS's in small electronic devices. Finally in Sec. V we give a short summary and discuss our results.

II. GENERAL NETWORK MODEL

A. Hamiltonian and spectrum

We start by giving a brief description of our quantum-network model; more details can be found in Ref. [20]. Identical localized quantum subsystems represent network nodes that are linked together by interactions. The network Hamiltonian thus has the general form

$$\hat{H}=\sum_{n=1}^{N}\hat{H}_n+\tfrac{1}{2}\sum_{\substack{n,m=1\\ n\neq m}}^{N}\hat{H}_{nm} \ . \tag{2.1}$$

The isolated subsystem n is characterized by its (relevant) spectrum consisting of I levels,

$$\hat{H}_n=\sum_{i_n=1}^{I}E^0_{i_n}|i_n\rangle\langle i_n| \ . \tag{2.2}$$

The network structure is embodied in the spatial arrangement of the subsystems and the interaction $\hat{H}_{nm}$. Here, we consider the following energy renormalization between subsystem n and m:

$$\hat{H}_{nm}=\sum_{i_n,i_m=1}^{I}V^{nm}_{i_n i_m}|i_n,i_m\rangle\langle i_n,i_m| \ . \tag{2.3}$$

Without loss of generality we assume $V^{nm}_{i_n i_m}=V^{mn}_{i_m i_n}$. This diagonal interaction will be shown to be generic for the cooperative stochastic dynamics that is exhibited when the network is coupled to the environment (e.g., heat bath or optical fields). In Sec. III we will give examples for physical systems that are approximately described by this network model.

The product states

$$|\{i_n\}\rangle=|i_1,i_2,\ldots,i_N\rangle=|i_1\rangle\otimes|i_2\rangle\otimes\cdots\otimes|i_N\rangle \tag{2.4}$$

that form a ($M=I^N$)-dimensional basis in the state space of the network diagonalize the network Hamiltonian (2.1),

$$\hat{H}|\{i_n\}\rangle=E_{\{i_n\}}|\{i_n\}\rangle \ . \tag{2.5}$$

The corresponding eigenvalues are

$$E_{\{i_n\}}=\sum_{n=1}^{N}E^0_{i_n}+\tfrac{1}{2}\sum_{\substack{n,m=1\\ n\neq m}}^{N}V^{nm}_{i_n i_m} \ . \tag{2.6}$$

B. Coupling to environment: Stochastic dynamics

In this section we derive the stochastic dynamics that is performed by the network when it is coupled to the environment (e.g., heat bath or light field). Stochastic quantum dynamics can only occur in open systems: The dynamics of an isolated system is completely described by the continuous time development of the Schrödinger or Liouville equation; once the initial conditions are given, there is no room left for any freedom of choice which could allow for "quantum jumps." As is well known, however, this completeness does not, in general, carry over to any subsystem: a truly nonclassical feature [26].

An ensemble of open quantum systems is conveniently described by a generalized master equation for the reduced density matrix [21]. This equation is derived in a standard way by starting with the Liouville equation of the closed entire system (quantum system + environment) and tracing out the irrelevant degrees of freedom of the environment [21]. For an incoherent interaction with the environment, which we will exclusively study here, the generalized master equation reduces to a simple rate equation (Pauli master equation) for the diagonal density-matrix elements [27]. The environment then simply shows up in transition rates between the eigenstates of the isolated quantum system.

The eigenstates of the quantum network are the product states $\{i_n\}$ (2.4). We restrict ourselves to environment-induced transitions between any two states $\{i_n\}$ and $\{j_n\}$, which differ in exactly one position, i.e.,

$$\begin{aligned}\{i_n\}&=\{i_1,i_2,\ldots,i_{m-1},i_m,i_{m+1},\ldots,i_N\} \ ,\\ \{j_n\}&=\{i_1,i_2,\ldots,i_{m-1},j_m,i_{m+1},\ldots,i_N\} \ .\end{aligned} \tag{2.7}$$

The transition energy between such two states is

$$\begin{aligned}\hbar\omega_{i_m j_m}(\{i_n\}')&=E_{\{i_1,i_2,\ldots,i_{m-1},j_m,i_{m+1},\ldots,i_N\}}\\ &\quad-E_{\{i_1,i_2,\ldots,i_{m-1},i_m,i_{m+1},\ldots,i_N\}}\\ &=\hbar\omega^0_{i_m j_m}+\sum_{\substack{n=1\\ n\neq m}}^{N}(V^{mn}_{j_m i_n}-V^{mn}_{i_m i_n}) \ ,\end{aligned} \tag{2.8}$$

which may be interpreted as a renormalized transition energy between the states j_m and i_m of subsystem m, depending on the neighborhood $\{i_n\}'=\{i_n,n\neq m\}$. $\hbar\omega^0_{i_m j_m}=E^0_{j_m}-E^0_{i_m}$ is the transition energy for the isolated subsystem. The Pauli master equation of the open quantum network then takes the form [20]

$$\frac{d}{dt}\rho(i_1,i_2,\ldots,i_N;t)=\sum_{m=1}^{N}\sum_{j_m=1}^{I}[R_{i_m j_m}(\{i_n\}')\rho(i_1,i_2,\ldots,i_{m-1},j_m,i_{m+1},\ldots,i_N;t)$$
$$-R_{j_m i_m}(\{i_n\}')\rho(i_1,i_2,\ldots,i_{m-1},i_m,i_{m+1},\ldots,i_N;t)]\ . \tag{2.9}$$

$\rho(\{i_n\};t)$ is a diagonal element of the network density matrix. The rate $R_{i_m j_m}(\{i_n\}')$ for the transition $j_m \to i_m$ might depend on the states of all other subsystems $\{i_n\}'$ as the transition frequency $\omega_{i_m j_m}(\{i_n\}')$ is—due to the diagonal interaction—a function of the states of the other subsystems. This is the origin of a complex network dynamics: If the interaction between the subsystems vanished, the Pauli master equation (2.9) would reduce to a set of independent rate equations for each subsystem.

The diagonal density-matrix elements $\rho(\{i_n\};t)$ in the Pauli master equation (2.9) still evolve continuously in time and therefore do not describe the stochastic dynamics of the open quantum system. This is not surprising since the density matrix describes a "mathematical" ensemble, i.e., a hypothetical infinite ensemble of identical copies, and not a single system: A diagonal density-matrix element gives the probability to find an arbitrary ensemble member in the corresponding state. Nevertheless, stochastic dynamics can now easily be derived from this rate equation if one interprets the associated Markoff process as the "real" dynamics of the single system [10]: This process $\{i_n(t)\}$ is a "random hopping" in state space, $\{i_n\}$, defined by the "hopping" rates $R_{i_m j_m}(\{i_n\}')$. This interpretation is consistent with the ensemble interpretation of the Pauli master equation: The superposition of different realizations $\{i_n(t)\}^l$, $l=1,2,\ldots,L$ of the Markoff process gives the correct ensemble limit [28,29]

$$\rho(\{i_n\};t)=\lim_{L\to\infty}\frac{1}{L}\sum_{l=1}^{L}\prod_{n}\delta_{i_n,i_n^l(t)}\ , \tag{2.10}$$

where the stochastic dynamics ("quantum noise") is eliminated. Some limitations for the stochastic interpretation are discussed in [10].

III. PHYSICAL REALIZATION OF QUANTUM NETWORKS

A. Interacting two-level defects in a heat bath

The single defect n is described by a two-level system (states $s_n=\pm1$, energy spacing ΔE). With an additional linear coupling to a static external field F [e.g., gate voltage in a metal-oxide-semiconductor field-effect transistor (MOSFET) [4]) we get for the local energies entering Eq. (2.2),

$$E_{s_n}^0=\left[\frac{\Delta E}{2}-\alpha F\right]s_n\ . \tag{3.1}$$

α is the coupling constant to the external field F. For convenience, we use the "spin variable" $s_n=\pm1$ instead of labeling the states by natural numbers as in (2.2).

We now consider a one-dimensional chain of identical defects with nearest-neighbor interaction that leads to an energy decrease (increase) of amount J if the two neighbors are in the same (opposite) state, i.e., the only nonvanishing matrix elements in Eq. (2.3) are

$$V_{s_n,s_{n+1}}^{n,n+1}=V_{s_{n+1},s_n}^{n+1,n}=-Js_n s_{n+1}\ . \tag{3.2}$$

Both the coupling to the external field and the interaction among the defects might be realized by different static dipole moments of the two states s_n. This model is equivalent to the one-dimensional Ising model with magnetic field $H=\alpha F-\Delta E/2$ and exchange interaction J. $J>0$ means "ferromagnetic"- and $J<0$ "antiferromagnetic"-type coupling. The eigenenergies (2.6) are

$$E_{\{s_n\}}=-H\sum_{n=1}^{N}s_n-J\sum_{n=1}^{N}s_n s_{n+1}\ . \tag{3.3}$$

For the transition energies (2.8) we get

$$\hbar\omega_{s_m}(\{s_n\}')=E_{\{s_1,s_2,\ldots,s_{m-1},s_m,s_{m+1},\ldots,s_N\}}-E_{\{s_1,s_2,\ldots,s_{m-1},-s_m,s_{m+1},\ldots,s_N\}}$$
$$=-2Hs_m-2Js_m(s_{m+1}+s_{m-1})\ . \tag{3.4}$$

The coupling to a heat bath leads to spontaneous "spin flips" $s_m\to-s_m$ with a rate $R_{s_m}(\{s_n\}')$. As it is unmistakable, $\omega_{s_m}(\{s_n\}')$ and also the transition rate $R_{s_m}(\{s_n\}')$ need only the one subscript s_m. The dynamics of this "kinetic Ising model" is governed by the rate equation (2.9) specialized to [30]

$$\frac{d}{dt}\rho(s_1,s_2,\ldots,s_N;t)=\sum_{m=1}^{N}[R_{-s_m}(\{s_n\}')\rho(s_1,s_2,\ldots,s_{m-1},-s_m,s_{m+1},\ldots,s_N;t)$$
$$-R_{s_m}(\{s_n\}')\rho(s_1,s_2,\ldots,s_{m-1},s_m,s_{m+1},\ldots,s_N;t)]\ . \tag{3.5}$$

The principle of detailed balance that holds for systems in thermal equilibrium [31] states that each term in the brackets on the right-hand side of (3.5) vanishes individually in the stationary case,

$$R_{-s_m}(\{s_n\}')\rho(s_1,s_2,\ldots,s_{m-1},-s_m,s_{m+1},\ldots,s_N)=R_{s_m}(\{s_n\}')\rho(s_1,s_2,\ldots,s_{m-1},s_m,s_{m+1},\ldots,s_N)\ . \tag{3.6}$$

On the other hand, the stationary state (thermal equilibrium) is characterized by a Boltzmann distribution. Thus, without modeling the heat bath in detail, Eq. (3.6) determines the ratio of the transition rates

$$\frac{R_{-s_m}(\{s_n\}')}{R_{s_m}(\{s_n\}')}=\exp\left[-\frac{\hbar\omega_{s_m}(\{s_n\}')}{k_BT}\right]=\exp\left[\frac{2}{k_BT}s_m[H+J(s_{m-1}+s_{m+1})]\right] . \tag{3.7}$$

A possible choice for $R_{s_m}(\{s_n\}')$ consistent with Eq. (3.7) is the familiar Glauber model [30,32]

$$R_{s_m}(\{s_n\}')=\frac{1}{2\tau_0}\left[1-\tanh\left[\frac{1}{k_BT}s_m[H+J(s_{m+1}+s_{m-1})]\right]\right] . \tag{3.8}$$

The parameter τ_0 determines the time scale of the dynamic process. As the transition rates only depend on the two next neighbors, we use the notation $R_{s_m}(s_{m-1},s_{m+1})$. The stochastic dynamics $\{s_m(t)\}$ becomes observable if the two states $s_m=-1$ and $s_m=+1$ are connected—via the associated electrostatic field—with the control of different electric current states.

B. Charge-transfer quantum-dot array in an incoherent electromagnetic field

Synthetic quantum networks should allow for more detailed structural and dynamical control. Here we study an array of charge-transfer quantum dots [33] (Fig. 1) coupled via their dipole-dipole interaction [34] as a prototype system [19]. Quantum dots with such complex internal structure have not yet been realized. However, two-dimensional quantum-well structures of that type [35] or simpler zero-dimensional quantum dots [16–18] are already under experimental control.

The relevant spectrum of a charge-transfer quantum dot consists of $I=3$ levels (see Fig. 1): The highest valence-band states 1 and 2 are localized within different potential wells; the lowest state in the conducting band 3 is delocalized over the whole dot. The Fermi level has to be pinned between level 1 and the higher level 2 to allow for an optically induced charge transfer between states 1 and 2 via the transient state 3. The specific spatial localization of the three states is associated with different static dipole moments [34]

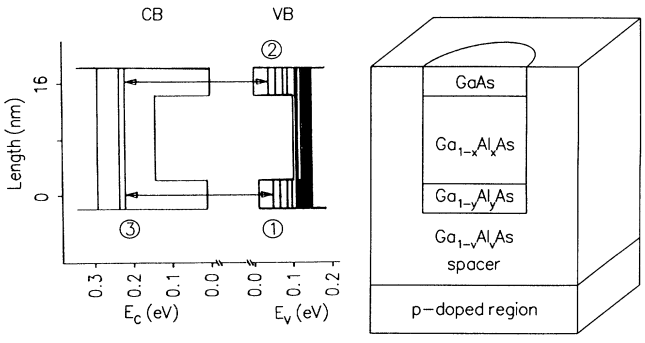

FIG. 1. Charge-transfer quantum dot and its spectrum. An asymmetric double-well potential is shaped in the valence band (VB) and conducting band (CB). In the ground state, level 1 is occupied and level 2 is free. Parameters $v=0.4$, $x=0.2$, $y=0.01$.

$$\mathbf{d}_2=-\mathbf{d}_1=d\mathbf{e}_z,\quad \mathbf{d}_3=\mathbf{0} . \tag{3.9}$$

$\mathbf{e}_z$ points in the axial direction of the dot.

The dominant part of the interaction $\hat{H}_{nm}$ between two quantum dots is the dipole-dipole term [34]

$$V_{i_n i_m}^{nm}=\frac{1}{4\pi\epsilon\epsilon_0|\mathbf{R}_{nm}|^3}\times\left[\mathbf{d}_{i_n}\cdot\mathbf{d}_{i_m}-\frac{3}{|\mathbf{R}_{nm}|^2}(\mathbf{R}_{nm}\cdot\mathbf{d}_{i_n})(\mathbf{R}_{nm}\cdot\mathbf{d}_{i_m})\right] . \tag{3.10}$$

$\mathbf{R}_{nm}$ is the separation vector between the two dots and ϵ the relative dielectric constant of the embedding semiconductor material.

The coupling to the electromagnetic field leads to transitions $j_m\rightarrow i_m$ in subsystem m with a rate

$$R_{i_m j_m}(\{i_n\}')=W_{i_m j_m}+B_{i_m j_m}U(\omega_{i_m j_m}(\{i_n\}')) . \tag{3.11}$$

$W_{i_m j_m}$ is the spontaneous and $B_{i_m j_m}U(\omega_{i_m j_m}(\{i_n\}'))$ the induced transition rate. $B_{i_m j_m}=B_{j_m i_m}$ are the Einstein coefficients and $U(\omega)$ the spectral energy density of the electromagnetic field. $W_{i_m j_m}$ is zero for $\omega_{i_m j_m}(\{i_n\}')<0$, i.e., $W_{21}=W_{31}=W_{32}=0$.

The specific structure of the quantum dot is connected with a hierarchy in the spontaneous transition rates due to the small overlap between states 1 and 2 ("localization selection rules") [33]. For our prototype quantum dot typical orders of magnitude are [36]

$$W_{13}\approx W_{23}\approx 10^8\ \mathrm{s}^{-1} ,\qquad W_{12}\approx 10\ \mathrm{s}^{-1} . \tag{3.12}$$

In the following we will set $W_{12}=0$. Typical values for the transition energies are [34]

$$\hbar\omega_{13}^0\approx\hbar\omega_{23}^0\approx 1\ \mathrm{eV} ,\qquad \hbar\omega_{12}^0\approx 10\ \mathrm{meV} , \tag{3.13}$$

and for the dipole-dipole interaction (3.10) [34]

$$V_{11}^{nm}=V_{22}^{nm}=-V_{12}^{nm}=-V_{21}^{nm}\approx 0.01\ \mathrm{meV} \tag{3.14}$$

for two quantum dots n and m with dipole moment $d\approx 8$ e nm (see Fig. 1), axial direction $\mathbf{e}_z$ perpendicular to the separation $\mathbf{R}_{nm}$ with $|\mathbf{R}_{nm}|=100$ nm, and $\epsilon=12$.

Restricting ourselves to the essentials of the charge-transfer dynamics defined by Eq. (2.9) we assume an electromagnetic field that fulfills the condition

$$B_{i_m j_m} U(\omega_{i_m j_m}(\{i_n\}')) \ll W_{13}, W_{23} \tag{3.15}$$

for all possible neighborhoods $\{i_n\}'$ and $i_m j_m = 13, 31, 23, 32$. A direct light field coupling between the two states 1 and 2 can be neglected. The hierarchy (3.15) implies an immediate decay of the transient state 3 after excitation. With an adiabatic elimination procedure the corresponding rate equation (2.9) then reduces to an effective rate equation with only two states per subsystem (see Appendix A). If we introduce the new nomenclature

$$(\text{state } 1) \hat{=} s = -1, \quad (\text{state } 2) \hat{=} s = +1 , \tag{3.16}$$

this effective rate equation has the same form as (3.5) with the effective rates

$$R_{s_m}(\{s_n\}') = \frac{\overline{W}_{-s_m}}{\overline{W}_1 + \overline{W}_{-1}} \overline{B}_{s_m} U(\overline{\omega}_{s_m}(\{s_n\}')) \tag{3.17}$$

for the transitions $s_m \rightarrow -s_m$. In order not to get confused with the parameters of the first model, we have labeled the following abbreviations with a bar:

$$\begin{aligned} &W_{13} := \overline{W}_{-1} , \\ &W_{23} := \overline{W}_1 , \\ &B_{13} = B_{31} := \overline{B}_{-1} , \\ &B_{23} = B_{32} := \overline{B}_1 , \\ &\omega_{13} = -\omega_{31} := \overline{\omega}_{-1} , \\ &\omega_{23} = -\omega_{32} := \overline{\omega}_1 . \end{aligned} \tag{3.18}$$

Especially note that $\overline{W}_s$ and $\overline{\omega}_s$ denote transitions from the transient state of the three-level model to the state s, whereas W_s and ω_s belong to the transition $s \rightarrow -s$. From (3.9) and (3.10) we get for the renormalized transition frequency (2.8)

$$\overline{\omega}_{s_m}(\{s_n\}') = \overline{\omega}^0_{s_m} - \sum_{\substack{n=1 \\ n \neq m}}^{N} C_{mn} s_m s_n , \tag{3.19}$$

with

$$\begin{aligned} C_{mn} &= C_{nm} \\ &= \frac{d^2}{4\pi\hbar\epsilon\epsilon_0 |\mathbf{R}_{nm}|^3} \\ &\quad \times \left[\mathbf{e}_z^n \cdot \mathbf{e}_z^m - \frac{3}{|\mathbf{R}_{nm}|^2} (\mathbf{R}_{nm} \cdot \mathbf{e}_z^n)(\mathbf{R}_{nm} \cdot \mathbf{e}_z^m) \right] . \end{aligned} \tag{3.20}$$

The reduction of the stochastic dynamics to a lower-dimensional state space (here from three to two) has been possible as a consequence of the time-scale splitting, leading to effective transitions composed of "elementary" transitions. In other scenarios concerning single quantum systems [1,25] such a time-scale splitting is exploited to observe the stochastic signal. Elementary states, coupled by a "probing" light field combine to "effective" states that are connected with different luminescence intensities. The stochastic signal in this reduced effective state space is thus mapped onto the luminescence intensity. Interpreting our states $s_m = \pm 1$ as such effective states gives the possibility to directly observe the stochastic signal $\{s_m(t)\}$ in this network realization.

To conclude, the stochastic dynamics of our two quantum-network realizations is described by the same type of rate equation (3.5), though with different expressions for the transition rates (3.8) and (3.17), respectively. The transition rates in the optically driven quantum-dot array can, in principle, be adjusted at will as a function of the transition frequencies $\omega_{s_m}(\{s_n\}')$ by the spectral energy density of the driving light field. The first model in thermal equilibrium is restricted in its dynamical repertoire by the condition of detailed balance (3.7) and controllable only by two parameters, temperature T and static external field F. Observation of the stochastic signal $\{s_m(t)\}$ exploits the fact that the physical properties of state $s_m = -1$ and $s_m = +1$ are different, being connected, e.g., with a high (low) current state or two different luminescence intensities.

IV. RANDOM TELEGRAPH SIGNALS

The stochastic quantum dynamics can be observed only in very refined experiments. The reason is that large systems are usually approximations of a "mathematical ensemble" (i.e., their Hamiltonian can be written as a sum of noninteracting identical Hamiltonians) in which the "quantum noise" is eliminated. A simple example is a gas of atoms whose interaction can be neglected. Stochastic dynamics will thus be observed only in very small systems (where the ensemble consists of only a few or even one member) or in larger systems where a certain intersubsystem interaction leads to cooperative dynamics and prevents the system from approximating a "mathematical" ensemble. Experimental examples for the first case are, e.g., single ions in a Paul trap [1–3] or single defects in a solid matrix [12,13,37]. The second case seems to be realized in very small tunnel junctions where large-amplitude current fluctuations are explained by a correlated defect dynamics [6]. Our quantum-network model even shows how a transition between a single system and ensemble behavior may be controlled by the environment.

A. Isolated subsystem: Normal RTS's

For an isolated subsystem, Eq. (3.5) reduces to

$$\frac{d}{dt}\rho(s;t) = R_{-s}\rho(-s;t) - R_s \rho(s;t), \quad s = \pm 1 \tag{4.1}$$

with

$$R_s = \frac{1}{2\tau_0} \left[1 - s \tanh\left(\frac{H}{k_B T} \right) \right] \tag{4.2}$$

for the thermal model (3.8) and

$$R_s = \frac{\overline{W}_{-s}}{\overline{W}_1 + \overline{W}_{-1}} \overline{B}_s U(\overline{\omega}_s^0) \tag{4.3}$$

for the optical model (3.17).

The corresponding Markoff process is a random hopping between the two states $s = \pm 1$ with hopping rates R_s. A computer simulation is shown in Fig. 2. This "normal" [7] two-level signal is characterized by an exponential decay of the correlation function

$$\langle s(t)s(t+\tau)\rangle = \left[\frac{R_{-1}-R_1}{R_{-1}+R_1}\right]^2 + \frac{4R_{-1}R_1}{(R_{-1}+R_1)^2} \times \exp[-(R_{-1}+R_1)|\tau|] \, . \tag{4.4}$$

This result is valid for the stationary case, where the correlation function does not depend on the absolute time t but only on the time difference τ. Usually observed two-level RTS's, as, e.g., in fluorescence intensity [1] or electric current [9], are normal RTS's, and one is thus lead to the conclusion that the underlying quantum dynamics is a stochastic two-point process. However, as will be shown in the next section, cooperation between single quantum systems may lead to "anomalous" two-level RTS's, as found, e.g., in small MOSFET's [14].

B. Two interacting subsystems: Minimal model for complex RTS's

We consider two coupled subsystems as a minimal model for more complex stochastic dynamics beyond normal RTS's. The dynamics of this network proceeds in a four-dimensional state space and can be visualized easily (see Fig. 3). It is defined by four transition rates $R_{s_1}(s_2)$ $(s_1, s_2 = \pm 1)$.

For our optically driven model (3.17) the corresponding four transition frequencies are $\overline{\omega}_{s_1}(s_2) = \overline{\omega}_{s_1}^0 - C_{12} s_1 s_2$, as shown in Fig. 4. We assume that they are all different and that the rates can be adjusted independently by the spectral energy density function $U(\omega)$. Within this large parameter space we restrict ourselves to the case

$$\begin{aligned} R_1(-1) &= R_{-1}(1) := \kappa_1 \, , \\ R_1(1) &= R_{-1}(-1) := \kappa_2 \, . \end{aligned} \tag{4.5}$$

For $\kappa_1 > \kappa_2$ we have a "ferromagnetic" coupling of the two subsystems as can be visualized in Fig. 3 where the thickness of the arrows denotes the magnitude of the transition rates. The two subsystems tend to stay in the same state in this case. As immediately seen from this figure, the condition of detailed balance is fulfilled for the choice (4.5): A necessary and sufficient condition is that the product of the transition rates over every closed loop in state space is equal for both directions [38]. Another evidence is that this choice of transition rates can be realized also by our thermal model: For $N = 2$ subsystems and $H = 0$ we get from (3.8)

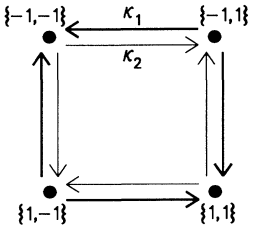

FIG. 3. Visualizing the stochastic dynamics of two coupled subsystems in the four-dimensional state space $\{s_1, s_2\}$. The thickness of the arrows indicates the magnitude of the transition rates. Ferromagnetic coupling for $\kappa_1 > \kappa_2$.

$$\begin{aligned} \kappa_1 &= \frac{1}{2\tau_0}\left[1 + \tanh\frac{J}{k_B T}\right] , \\ \kappa_2 &= \frac{1}{2\tau_0}\left[1 - \tanh\frac{J}{k_B T}\right] . \end{aligned} \tag{4.6}$$

Ferromagnetic coupling $\kappa_1 > \kappa_2$, here, is expressed by the more conventional statement $J > 0$.

Stochastic traces $s_1(t)$ and $s_2(t)$ are depicted in Fig. 5 for different parameters $\kappa_1/\kappa_2 \geq 1$. For $\kappa_1 = \kappa_2$ the two subsystems are not coupled and jump independently. Increasing the ratio κ_1/κ_2 leads to a correlation of jumps. For $\kappa_1 \gg \kappa_2$, the ferromagnetic order is established on the fast scale $1/\kappa_1$, which on the slow scale $1/\kappa_2$ looks as entrained jumps of the two subsystems. This result will be generalized in Sec. IV C to a chain of N subsystems.

Stationary correlation functions can be obtained by time averaging over the stochastic signal or directly by solving the corresponding master equation [30]. The result is

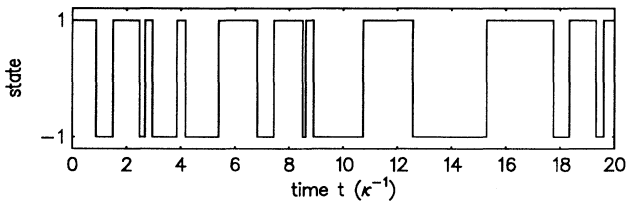

FIG. 2. Random telegraph signal $s(t)$ of an isolated subsystem. Parameters $R_{-1} = R_1 = \kappa$.

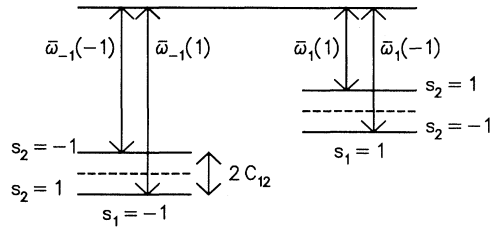

FIG. 4. Dipole-dipole renormalization of the unperturbed energy levels (dashed) of subsystem 1 due to subsystem 2.

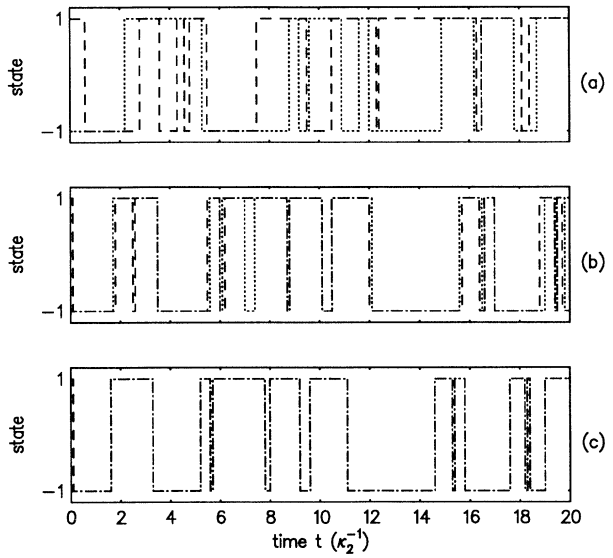

FIG. 5. Random telegraph signals $s_1(t)$ (dashed) and $s_2(t)$ (dotted) in two ferromagnetic-coupled subsystems. (a) $\kappa_1=\kappa_2$, (b) $\kappa_1=10\kappa_2$, (c) $\kappa_1=1000\kappa_2$.

$$\langle s_1(t)s_1(t+\tau)\rangle=\langle s_2(t)s_2(t+\tau)\rangle = \frac{\kappa_1}{\kappa_1+\kappa_2}\exp(-2\kappa_2|\tau|) + \frac{\kappa_2}{\kappa_1+\kappa_2}\exp(-2\kappa_1|\tau|)\ . \tag{4.7}$$

For $\kappa_1\neq\kappa_2$, the correlation in either subsystem no longer decays just exponentially, the RTS's are anomalous due to the coupling between the subsystems. The cross correlation between the two subsystems is

$$\langle s_1(t)s_2(t+\tau)\rangle = \frac{\kappa_1}{\kappa_1+\kappa_2}\exp(-2\kappa_2|\tau|) - \frac{\kappa_2}{\kappa_1+\kappa_2}\exp(-2\kappa_1|\tau|)\ . \tag{4.8}$$

For $\kappa_1>\kappa_2$ (ferromagnetic coupling) it is positive, for $\kappa_1<\kappa_2$ (antiferromagnetic coupling) it is negative, and for $\kappa_1=\kappa_2$ it vanishes as expected for any τ. For $\tau=0$ and in the limit $\kappa_1\gg\kappa_2$ we get maximal correlation $\langle s_1(t)s_2(t)\rangle=1$, in the limit $\kappa_1\ll\kappa_2$ maximal anticorrelation, $\langle s_1(t)s_2(t)\rangle=-1$. The fact that all correlation functions are a sum of exponentials is a consequence of the detailed balance condition. In this case the eigenvalues of the so-called relaxation matrix are all real [31]. For later reference we, finally, include the correlation function for the variable $S=s_1+s_2$, which is obtained from (4.7) and (4.8),

$$\langle S(t)S(t+\tau)\rangle=\frac{4\kappa_1}{\kappa_1+\kappa_2}\exp(-2\kappa_2|\tau|)\ . \tag{4.9}$$

C. Linear chain: Large-amplitude RTS's

We examine the stochastic dynamics of a linear chain of localized two-level systems with nearest-neighbor interaction. Figure 6 shows stationary sample traces for the macrovariable $S(t)=\sum_{n=1}^{N}s_n(t)$ and the thermal transition-rate model (3.8) with periodic boundary conditions, $N=10$, $H=0$, and different values J/k_BT. For $J/k_BT=0$ the transition rate $R_{s_m}(s_{m-1},s_{m+1})$ does not depend on the state of the two neighbors and each subunit changes its state independently. Increasing J/k_BT (ferromagnetic coupling) leads to a cooperative dynamics of the subunits. The fluctuations become larger and for large enough J/k_BT only two-state fluctuations between the extrema $S=\pm N$ remain. The increase of the relevant time scale as seen in Fig. 6 will be explained by Eq. (4.24).

If we assume that any transition $s_m\rightarrow -s_m$ of a defect induces the same current change, the RTS of the current should map linearly upon the macrovariable $S(t)$. Note the striking similarity between these simulations and their temperature dependence with the observed current fluctuations [6]. A comparison of the qualitative behavior leads to an estimate of our model parameter J. Here we obtain as an order of magnitude $J\approx 10$ meV. Of course, strictly speaking, only time averages as correlations functions should be compared and not time sections of a realization of the stochastic process itself. Therefore,

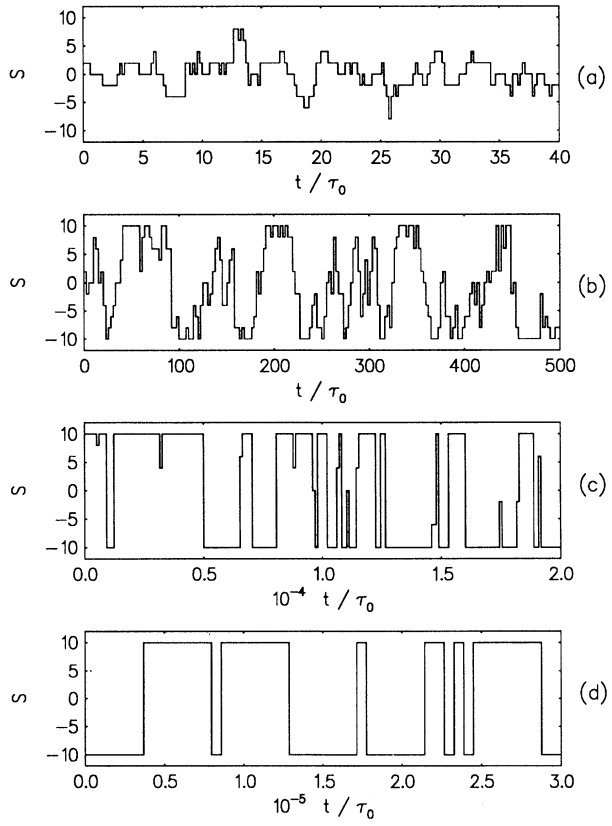

FIG. 6. Sample traces $S(t)=\sum_{n=1}^{N}s_n(t)$ for the stochastic model (3.8). Chain length $N=10$, external field $H=0$. (a) $J/k_BT=0$, (b) $J/k_BT=0.8$, (c) $J/k_BT=1.6$, (d) $J/k_BT=2.4$. Transition from uncorrelated noise to cooperative two-level fluctuations.

much more experimental data are needed.

Figure 7 shows on ever finer time scales how this large-amplitude two-level signal emerges on a coarse-grained scale as a consequence of correlated jumps of the single subsystems. For $H \neq 0$, this large-amplitude RTS becomes asymmetric (Fig. 8), which also will be explained by Eq.(4.24).

The stationary correlation function $\langle S(t)S(t+\tau)\rangle$ can be calculated from the time-dependent solution of the rate equation (3.5) [30],

$$\langle S(t)S(t+\tau)\rangle = \sum_{\{s_n\}} \sum_{\{s_n'\}} SS'\rho(\{s_n\})\rho(\{s_n'\};\tau) \tag{4.10}$$

with $S=\sum_n s_n$ and $S'=\sum_n s_n'$. As above, $\rho(\{s_n\})$ is the stationary solution of the rate equation. $\rho\{s_n'\};\tau)$ is the time-dependent solution for the initial condition $\rho(\{s_n'\};0)=\prod_n \delta_{s_n s_n'}$; it can be interpreted as the conditional probability that the system is in the state $\{s_n'\}$ at time τ if it was in state $\{s_n\}$ at time 0. For $H=0$, the sum over $\{s_n'\}$ in (4.10) can be calculated analytically [30],

$$\sum_{\{s_n'\}} S'\rho(\{s_n'\};\tau) = S\exp\left[-(1-\gamma)\frac{|\tau|}{\tau_0}\right], \tag{4.11}$$

with $\gamma=\tanh(2J/k_BT)$. This sum is the time-dependent expectation value of the macrovariable S' that decays simply exponentially. Inserting this result into (4.10) gives

$$\begin{aligned}\langle S(t)S(t+\tau)\rangle &= \sum_{\{s_n\}} S^2\rho(\{s_n\})\exp\left[-(1-\gamma)\frac{|\tau|}{\tau_0}\right] \\ &= \langle S^2\rangle\exp\left[-(1-\gamma)\frac{|\tau|}{\tau_0}\right].\end{aligned} \tag{4.12}$$

Thus the noise spectrum of S, i.e., the Fourier transform of the correlation function (4.12), turns out to be a simple

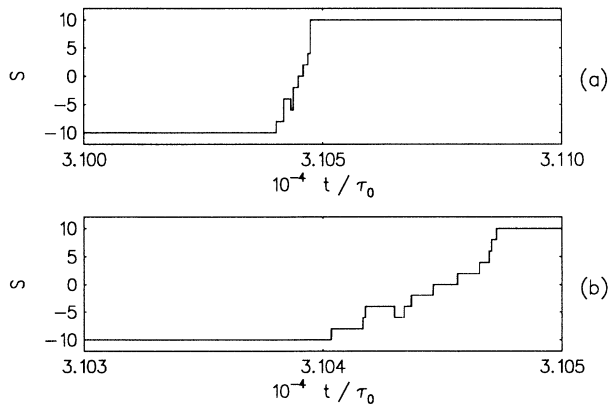

FIG. 7. Finer time scale of the first large-amplitude jump in Fig. 6(d). It is the result of a correlated stochastic dynamics of the subsystems on a faster time scale.

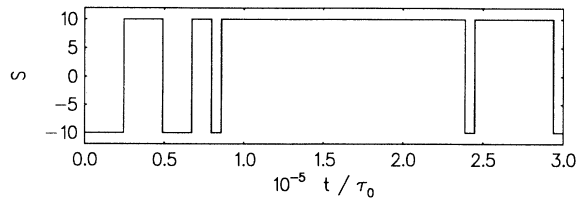

FIG. 8. Asymmetric large-amplitude two-level random telegraph signal. $H/J=0.02$, $J/k_BT=2.4$.

Lorentzian shape [7] of width $(1-\gamma)/\tau_0$ that decreases with increasing parameter J/k_BT. The expectation value $\langle S^2\rangle$ of the Ising chain with periodic boundary conditions can be calculated by means of the transfer matrix method [39]. The result is

$$\langle S^2\rangle = N\frac{(1-\eta^N)(1+\eta)}{(1+\eta^N)(1-\eta)} \tag{4.13}$$

with $\eta=\tanh(J/k_BT)$. As the stationary expectation value of S vanishes for $H=0$, $\langle S^2\rangle$ gives the mean-square deviation of S. For $J/k_BT=0$ ($\eta=0$) we obtain the result of N independent subsystems $\langle S^2\rangle=N$. In the limit $J/k_BT\to\infty$ ($\eta\to 1$), the fluctuations become as large as the system size N, i.e., $\langle S^2\rangle=N^2$. For $N=2$ and replacing J by $J/2$ (no periodic boundary conditions in Sec. IV B), Eq. (4.9) is recovered from (4.12) and (4.13).

Finally, by deriving an effective two-level rate equation we show that the large-amplitude two-level signal that emerges for large enough parameter J/k_BT again represents a normal RTS: The ensemble of correlated two-level subsystems behaves as a single two-level quantum system in this limit. For the case $H=0$, to which we restrict ourselves presently, the stationary probabilities $\rho(S=Ns)$ for the "macroscopic" states $\{s,s,\ldots,s\}$ ($s=\pm 1$) are [39]

$$\rho(N)=\rho(-N) = \frac{\exp\left[\frac{NJ}{k_BT}\right]}{\left[2\cosh\left[\frac{J}{k_BT}\right]\right]^N + \left[2\sinh\left[\frac{J}{k_BT}\right]\right]^N}. \tag{4.14}$$

The condition for the appearance of large-amplitude two-state fluctuations

$$1-[\rho(N)+\rho(-N)] \ll 1 \tag{4.15}$$

then turns out to be equivalent to

$$N \ll \xi, \tag{4.16}$$

with

$$\xi = -\left[\ln\tanh\left[\frac{J}{k_BT}\right]\right]^{-1}. \tag{4.17}$$

In the thermodynamic limit $N\to\infty$ ξ has the significance of a correlation length [39]

$$\langle s_m s_{m+r}\rangle = \exp\left[-\frac{r}{\xi}\right] . \tag{4.18}$$

As a consequence, large two-state fluctuations are observable in finite systems if the correlation length is larger than the system size N.

In conjunction with Eq. (3.8) condition (4.16) implies an order of magnitude splitting in the transition rates,

$$N^2 R_s(s,s), N^2 R_{-s}(-s,-s) \ll R_s(-s,s), R_s(-s,-s), R_{-s}(-s,s), R_{-s}(s,s) . \tag{4.19}$$

Here, only $H \ll J$ has to be presumed. The hierarchy (4.19) is the analog on to the condition $\kappa_2 \ll \kappa_1$ in Sec. IV B. Equation (4.19), in turn, allows an adiabatic elimination procedure in Eq. (3.5) resulting in the desired two-state rate equations for the macroscopic states $S = Ns$ (see Appendix B),

$$\frac{d}{dt}\rho(Ns;t) = R^{\text{eff}}_{-Ns}\rho(-Ns;t) - R^{\text{eff}}_{Ns}\rho(Ns;t) . \tag{4.20}$$

The effective transition rates R^{eff}_{Ns} are

$$R^{\text{eff}}_{Ns} = \frac{2N\Lambda(s)R_s(s,s)R_s(-s,-s)[R_s(-s,s)-R_{-s}(-s,s)]}{R_s(-s,-s)\Gamma(s)\Lambda(s) - R_{-s}(s,s)\Gamma(-s)\Lambda(-s)} , \tag{4.21}$$

where

$$\Gamma(s) = R_{-s}(s,s) + 2[R_s(-s,s) - R_{-s}(-s,s)] \tag{4.22}$$

and

$$\Lambda(s) = \left[\frac{R_s(-s,s)}{R_{-s}(-s,s)}\right]^{N/2-1} . \tag{4.23}$$

$\tau_{Ns} = 1/R^{\text{eff}}_{Ns}$ is the mean time spent in the state Ns. Figure 9 compares the results for τ_{Ns} from our simulations with the adiabatic approximation (4.21) and shows excellent agreement. For $N|H|/k_BT \ll 1$ we obtain from (4.21) with the transition-rate model (3.8)

$$\tau_{Ns} = \tau_0 \exp\left[\frac{4J + NsH}{k_BT}\right] . \tag{4.24}$$

The exponential temperature and external-field dependence of this model perfectly agrees with experimental observation [4] for $\tau_0 \approx 10^{-6}$ s and $J \approx 10$ meV; the system size N and the other parameters ΔE and α would have to be obtained from more detailed experimental data. Whereas this exponential dependence is usually explained as a thermally activated switching of a single defect state [7,40] (i.e., by a temperature dependence of parameter τ_0), here it is a consequence of the interaction among the defects.

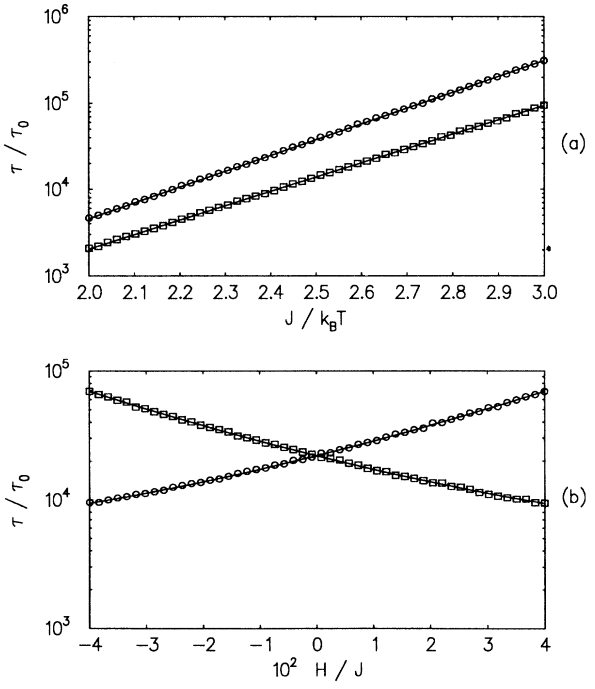

FIG. 9. Mean time $\tau_{\pm N}$ spent in the macroscopic states $S = \pm N$. Comparison of the simulations ($\circ, \tau_{+N}$; $\square, \tau_{-N}$) with the adiabatic result (solid line) (a) as a function of J/k_BT with $\mu H/J = 0.02$, and (b) as a function of H/J with $J/k_BT = 2.5$.

Finally, we show how the thermal realization (3.8) can be "simulated" by the optical one. At first sight, the long-range dipole-dipole interaction (3.20) seems to prevent such a mapping as the transition rate (3.8) depends only on the three possible states $s_{m+1} + s_{m-1} = 0, \pm 1$ of the two nearest neighbors. However, Eq. (3.19) defines for each of the two values $s_m = \pm 1$ three nonoverlapping frequency bands where the central frequencies given by the next neighbors are separated by $\Delta\omega = 2C_0$ (nearest-neighbor dipole-dipole interaction C_0) and all other subsystems form the "inhomogeneous" bandwidth $\delta\omega = 4C_0 \sum_{n=2}^{\infty} 1/n^3 \approx 0.808 C_0$ (cf. Fig. 10). If, additionally, the unperturbed transition frequencies $\bar{\omega}^0_1$ and $\bar{\omega}^0_{-1}$ are separated well enough,

$$|\bar{\omega}^0_1 - \bar{\omega}^0_{-1}| > 2\Delta\omega + \delta\omega \approx 4.808 C_0 , \tag{4.25}$$

all six frequency bands mutually do not overlap and the six transition rates depending only on the states of the nearest neighbors

$$R_s(s,s), R_s(-s,-s), R_s(-s,s) = R_s(s,-s) , \quad s = \pm 1 \tag{4.26}$$

can then be adjusted independently by taking $U(\omega)$ to be constant over each frequency band. The optically driven

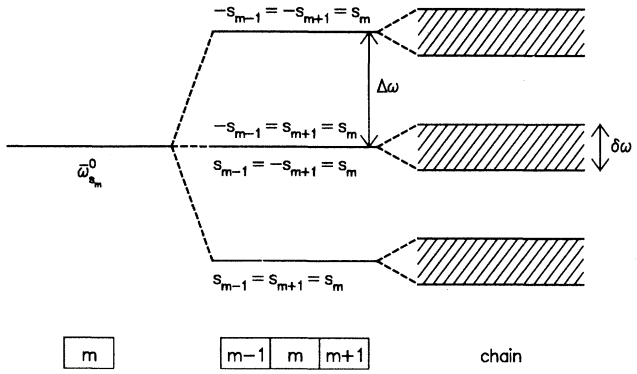

FIG. 10. Frequency renormalization in the linear chain. The two nearest neighbors lead to a splitting $\Delta\omega$ of the transition frequencies $\bar{\omega}^0_{s_m}$ of the isolated subsystem m. The other subsystems give the "inhomogeneous" bandwidth $\delta\omega$.

model may "simulate" the thermal model in this case. The orders of magnitude (3.13) and (3.14) show that the condition (4.25) is fulfilled for our model system. The signal $S(t)$ could be monitored in the resonance fluorescence signal caused by an additional "probe" light field (cf. Sec. III B).

V. SUMMARY AND DISCUSSION

Our quantum-network model is rather general and not based on a special scenario; it can be applied to driven systems and systems in thermal equilibrium alike. It demonstrates how large-amplitude few-level RTS's emerge through the cooperative dynamics in an ensemble of interacting quantum subunits. The main prerequisite for the emergence of correlated jumps is an order of magnitude difference in the transition rates (4.19) leading to a kind of avalanche dynamics. Those correlated jumps are a signature of mesoscopic quantum behavior in the sense that the underlying stochastic quantum dynamics becomes visible on the mesoscopic scale via a collective variable $S=\sum_n s_n$.

Our model can explain the appearance of low-temperature few-level fluctuations in the current noise of small tunnel junctions. The model parameters obtained by fitting the experimental data are of reasonable order of magnitude. Analogous effects in the optical properties of molecular-structured materials are predicted. The dynamical repertoire should even be larger in this driven system than in the thermal system, which is restricted by the detailed balance condition. In an array of charge-transfer quantum dots complex random telegraph noise and novel fluctuation phenomena should be controllable by an external light field. It should lead, e.g., to very unusual luminescence properties.

Only for simplicity and in order to demonstrate the generic nature have we focused on two states per subsystem and nearest-neighbor interaction; this has allowed us to exploit the otherwise superficial similarity with the Ising model. The appearance of large-amplitude RTS's does not sensitively rely on the translational invariance of our model nor on the periodic boundary conditions. Even spatial parameter fluctuations (to be expected in a defect gas [6]) will not destroy the two-level signal as long as the (now spatially dependent) transition rates obey Eq. (4.19). However, those fluctuations are expected to modify the noise spectrum. Preliminary numerical simulations for a two-dimensional lattice indicate that large RTS's are not restricted to one-dimensional models either: As the RTS occurs for conditions opposite to the thermodynamic limit, corresponding dimensionality effects as for phase transitions should not be expected.

ACKNOWLEDGMENT

This work has been supported by the Deutsche Forschungsgemeinschaft (Sfb 329).

APPENDIX A

The unequality (3.15) that implies an immediate decay of the transient state 3 after excitation leads to the following hierarchy in the occupation probabilities:

$$\rho(i_1,i_2,\ldots,i_N;t)\gg\rho(i_1,i_2,\ldots,i_{m-1},3,i_{m+1},\ldots,i_N;t)\gg\rho(i_1,i_2,\ldots,i_{l-1},3,i_{l+1},\ldots,i_{m-1},3,i_{m+1},\ldots,i_N;t)\gg\ldots, \tag{A1}$$

where the i_n, here, take only the values $i_n=1,2$. Each occupied state 3 reduces the occupation probability by one order. The system of rate equations (2.9) can then be approximated "up to first order" by

$$\frac{d}{dt}\rho(i_1,i_2,\ldots,i_N;t)=\sum_{m=1}^{N}[\,W_{i_m 3}\rho(i_1,i_2,\ldots,i_{m-1},3,i_{m+1},\ldots,i_N;t) - B^m_{i_m 3}U(\omega^m_{i_m 3}(\{i_n\}'))\rho(i_1,i_2,\ldots,i_{m-1},i_m,i_{m+1},\ldots,i_N;t)] \tag{A2}$$

for the elements containing no occupied level 3 and

$$\frac{d}{dt}\rho(i_1,i_2,\ldots,i_{m-1},3,i_{m+1},\ldots,i_N;t)=\sum_{j_m=1}^{2}[\,B^m_{j_m 3}U(\omega^m_{j_m 3}(\{i_n\}'))\rho(i_1,i_2,\ldots,i_{m-1},j_m,i_{m+1},\ldots,i_N;t) - W_{j_m 3}\rho(i_1,i_2,\ldots,i_{m-1},3,i_{m+1},\ldots,i_N;t)] \tag{A3}$$

for the elements containing exactly one occupied level 3. The hierarchy (3.15) allows us to adiabatically eliminate the "fast" variables $\rho(i_1,i_2,\ldots,i_{m-1},3,i_{m+1},\ldots,i_N;t)$ by setting the time derivative in Eq. (A3) equal to zero. The result is

$$\frac{d}{dt}\rho(i_1,i_2,\ldots,i_N;t)=\sum_{m=1}^{N}\left[\frac{W^m_{i_m 3}}{W^m_{13}+W^m_{23}}B^m_{\bar{i}_m 3}U(\omega^m_{\bar{i}_m 3}(\{i_n\}'))\rho(i_1,i_2,\ldots,i_{m-1},\bar{i}_m,i_{m+1},\ldots,i_N;t)\right.$$
$$\left.-\frac{W^m_{\bar{i}_m 3}}{W^m_{13}+W^m_{23}}B^m_{i_m 3}U(\omega^m_{i_m 3}(\{i_n\}'))\rho(i_1,i_2,\ldots,i_{m-1},i_m,i_{m+1},\ldots,i_N;t)\right], \tag{A4}$$

with $\bar{i}_m=3-i_m$. Introducing the new nomenclature (3.16) and (3.18) then leads to the more comprehensive form (3.5) with the effective rates (3.17).

APPENDIX B

The transition-rate hierarchy (4.19) means that the formation of a cluster that begins with the "flipping" of one subsystem in the homogeneous state is very unlikely. This implies, in turn, a hierarchy in the occupation probabilities

$$\rho(1,1,\ldots,1;t),\rho(-1,-1,\ldots,-1;t)$$
$$\gg\rho(1,1,\ldots,1,-1,-1,\ldots,-1,1,1,\ldots,1;t)$$
$$\gg\rho(1,1,\ldots,1,-1,-1,\ldots,-1,1,1,\ldots,1,-1,-1,\ldots,-1,1,1,\ldots,1;t)\gg\cdots . \tag{B1}$$

Each cluster reduces the occupation probability by about one order. Up to first order, the rate equations (3.5) can then be transcribed into rate equations for the probability $\rho(S;t)$ ($S=-N,-N+2,\ldots,N$) that the chain (periodic boundary conditions) consists of two clusters, one with $(N+S)/2$ subsystems in state 1 and the other with $(N-S)/2$ subsystems is state -1,

$$\frac{d}{dt}\rho(Ns;t)=R_{-s}(s,s)\rho((N-2)s;t)-NR_s(s,s)\rho(Ns;t)\ , \tag{B2}$$

$$\frac{d}{dt}\rho((N-2)s;t)=2R_{-s}(-s,s)\rho((N-4)s;t)+NR_s(s,s)\rho(Ns;t)$$
$$-[R_{-s}(s,s)+2R_s(-s,s)]\rho((N-2)s;t),\quad s=\pm 1 \tag{B3}$$

$$\frac{d}{dt}\rho(S;t)=2R_1(-1,1)\rho(S+2;t)+2R_{-1}(-1,1)\rho(S-2;t)$$
$$-2[R_{-1}(-1,1)+R_1(-1,1)]\rho(S;t),\quad S=-N+4,-N+6,\ldots,N-4\ . \tag{B4}$$

The variables $S=\pm N$ (B2) are slowly damped with $NR_s(s,s)$. The adiabatic solution $[d\rho(S;t)/dt=0]$ for the fast variables $S=-N+2,-N+4,\ldots,N-2$ is from (B3) and (B4),

$$\rho(S;t)=a(t)\left[\frac{R_{-1}(-1,1)}{R_1(-1,1)}\right]^{S/2}+b(t)\ , \tag{B5}$$

with

$$a(t)=N\frac{R_1(1,1)\Gamma(-1)\rho(N;t)-R_{-1}(-1,-1)\Gamma(1)\rho(-N;t)}{R_{-1}(1,1)\Gamma(-1)\Lambda(-1)-R_1(-1,-1)\Gamma(1)\Lambda(1)} \tag{B6}$$

and

$$b(t)=N\frac{R_{-1}(-1,-1)R_{-1}(1,1)\Lambda(-1)\rho(-N;t)-R_1(1,1)R_1(-1,-1)\Lambda(1)\rho(N;t)}{R_{-1}(1,1)\Gamma(-1)\Lambda(-1)-R_1(-1,-1)\Gamma(1)\Lambda(1)}\ . \tag{B7}$$

For the expressions for $\Gamma(s)$ and $\Lambda(s)$ see Eqs. (4.22) and (4.23). Inserting (B5) for $S=(N-2)s$ into Eq. (B2) eventually gives the two-level rate equation (4.20).

[1] W. Nagourney, J. Sandberg, and H. Dehmelt, Phys. Rev. Lett. **56**, 2797 (1986).
[2] Th. Sauter, W. Neuhauser, R. Blatt, and P. E. Toschek, Phys. Rev. Lett. **57**, 1696 (1986).
[3] J. C. Bergquist, R. G. Hulet, W. M. Itano, and D. J. Wineland, Phys. Rev. Lett. **57**, 1699 (1986).
[4] K. S. Ralls *et al.*, Phys. Rev. Lett. **52**, 228 (1984).
[5] T. Judd *et al.*, Appl. Phys. Lett. **49**, 1652 (1986).
[6] K. R. Farmer, C. T. Rogers, and R. A. Buhrman, Phys. Rev. Lett. **58**, 2255 (1987); K. S. Ralls and R. A. Buhrman, Phys. Rev. B **44**, 5800 (1991).
[7] M. J. Kirton and M. J. Uren, Adv. Phys. **38**, 367 (1989).
[8] M. O. Andersson *et al.*, Phys. Rev. B **41**, 9836 (1990).
[9] M. Schulz and A. Karmann, Phys. Scr. **T35**, 273 (1991).
[10] W. G. Teich and G. Mahler, Phys. Rev. A **45**, 3300 (1992).
[11] J. Dalibard, Y. Castin, and K. Molmer, Phys. Rev. Lett. **68**, 580 (1992).
[12] W. E. Moerner and L. Kador, Phys. Rev. Lett. **62**, 2535 (1989).
[13] W. P. Ambrose and W. E. Moerner, Nature **349**, 225 (1991).
[14] M. J. Uren, M. J. Kirton, and S. Collins, Phys. Rev. B **37**, 8346 (1988).
[15] W. H. Card and P. K. Chaudhari, Proc. IEEE **53**, 652 (1965).
[16] M. A. Reed *et al.*, Phys. Rev. Lett. **60**, 535 (1988).
[17] Ch. Sikorski and U. Merkt, Phys. Rev. Lett. **62**, 2164 (1989).
[18] T. Demel *et al.*, Phys. Rev. Lett. **64**, 788 (1990).
[19] G. Mahler, H. Körner, and W. Teich, in *Advances in Solid State Physics,* edited by U. Rössler, Festkörperprobleme Vol. 31 (Vieweg, Braunschweig, 1991), p. 357.
[20] H. Körner and G. Mahler (unpublished).
[21] K. Blum, *Density Matrix Theory and Applications* (Plenum, New York, 1981).
[22] A. Schenzle, R. G. DeVoe, and R. G. Brewer, Phys. Rev. A **33**, 2127 (1986).
[23] M. Porrati and S. Putterman, Phys. Rev. A **39**, 3010 (1989).
[24] R. J. Cook and H. J. Kimble, Phys. Rev. Lett. **54**, 1023 (1985).
[25] H. J. Kimble, R. J. Cook, and A. L. Walls, Phys. Rev. A **34**, 3190 (1986).
[26] B. d'Espagnat, *Conceptual Foundations of Quantum Mechanics* (Benjamin, Menlo Park, 1971).
[27] H. Haken, in *Laser Theory,* edited by S. Flügge, Encyclopedia of Physics Vol. XXV/2c (Springer, Berlin, 1970).
[28] F. Reif, *Fundamentals of Statistical and Thermal Physics* (McGraw-Hill, New York, 1965).
[29] N. G. van Kampen, *Stochastic Processes in Physics and Chemistry* (North-Holland, Amsterdam, 1981).
[30] R. J. Glauber, J. Math. Phys. **4**, 294 (1963).
[31] H. Haken, *Synergetics. An Introduction,* 3rd ed. (Springer, Berlin, 1983).
[32] M. Suzuki and R. Kubo, J. Phys. Soc. Jpn. **24**, 51 (1968).
[33] K. Obermayer, W. G. Teich, and G. Mahler, Phys. Rev. B **37**, 8096 (1988).
[34] W. G. Teich, K. Obermayer, and G. Mahler, Phys. Rev. B **37**, 8111 (1988).
[35] M. G. W. Alexander *et al.*, Appl. Phys. Lett. **55**, 885 (1989).
[36] K. Obermayer, G. Mahler, and H. Haken, Phys. Rev. Lett. **58**, 1792 (1987).
[37] M. Orrit and J. Bernard, Phys. Rev. Lett. **65**, 2716 (1990).
[38] *Interregional Migration,* edited by W. Weidlich and G. Haag (Springer, Berlin, 1988).
[39] H. E. Stanley, *Introduction to Phase Transitions And Critical Phenomena* (Clarendon, Oxford, 1971).
[40] C. T. Rogers and R. A. Buhrman, Phys. Rev. Lett. **55**, 859 (1985).